Effect of Adipocyte Secretome in Melanoma Progression and Vasculogenic Mimicry

Pedro Coelho,[1,2,3] Joana Almeida,[2,3] Cristina Prudêncio,[2,3] Rúben Fernandes,[2,3] and Raquel Soares[1,3]*

[1]*Department of Biochemistry, Faculty of Medicine, University of Porto, Porto, Portugal*

[2]*Ciências Químicas e Biomoléculas, Escola Superior de Tecnologia da Saúde do Porto, Instituto Politécnico do Porto, Porto, Portugal*

[3]*Instituto de Inovação e Investigação em Saúde, Universidade do Porto, Porto, Portugal*

*Correspondence to: Raquel Soares, Departamento de Bioquímica, Faculdade de Medicina da Universidade do Porto, Al. Prof. Hernˆani Monteiro, 4200-319 Porto, Portugal. E-mail: raqsoa@med.up.pt

ABSTRACT

Obesity, favored by the modern lifestyle, acquired epidemic proportions nowadays. Obesity has been associated with various major causes of death and morbidity including malignant neoplasms. This increased prevalence has been accompanied by a worldwide increase in cutaneous melanoma incidence rates during the last decades. Obesity involvement in melanoma aetiology has been recognized, but the implicated mechanisms remain unclear. In the present study, we address this relationship and investigate the influence of adipocytes secretome on B16-F10 and MeWo melanoma cell lines. Using the 3T3-L1 adipocyte cell line, as well as ex vivo subcutaneous (SAT) and visceral (VAT) adipose tissue conditioned medium, we were able to show that adipocyte-released factors play a dual role in increasing melanoma cell overall survival, both by enhancing proliferation and decreasing apoptosis. B16-F10 cell migration and cell–cell and cell–matrix adhesion capacity were predominantly enhanced in the presence of SAT and VAT released factors. Melanocytes morphology and melanin content were also altered by exposure to adipocyte conditioned medium disclosing a more dedifferentiated phenotype of melanocytes. In addition, exposure to adipocyte-secreted molecules induced melanocytes to rearrange, on 3D cultures, into vessel-like structures, and generate characteristic vasculogenic mimicry patterns. These findings are corroborated by the released factors profile of 3T3-L1, SAT, and VAT assessed by microarrays, and led us to highlight the mechanisms by which adipose secretome from sub-cutaneous or visceral depots promote melanoma progression.

KEY WORDS: OBESITY; MELANOMA; VASCULOGENIC MIMICRY; ADIPOSE TISSUE

Abbreviations used:
AT, adipose tissue;
CM, conditioned medium;
DMEM, Dulbecco′s modified eagle′s medium;
FBS, foetal bovine serum;
FGF, fibroblast growth factor;
HGF, hepatocyte growth factor;
HMEC-1, human microvascular endothelial cells;
IGF, insulin-like growth factor;
IGFBP, insulin-like growth factor binding protein;
IL, interleukin;
LIF, leukaemia inhibitory factor;
MCP-1, monocyte chemotactic protein 1;
PAI-1, plasminogen activator inhibitor-1;
PBS, phosphate buffered saline;
RBP-4, Retinol binding protein-4;
SAT, subcutaneous adipose tissue;
SEM, standard error of the mean;
TIMP, tissue inhibitor of metalloproteinases;
VAT, visceral adipose tissue;
VEGF, vascular endothelial growth factor.

Obesity prevalence has significantly increased worldwide [Rubenstein, 2005], leading to a public health concern and branded as "the modern epidemic" [Haffner and Taegtmeyer, 2003; Rubenstein, 2005]. The prevalence of obesity in Europe has increased by approximately 30% over the past 10 years and this phenomenon is corroborated by data from several other countries [Berghöfer et al., 2008]. It has long been recognized that excess adipose tissue (AT) increases the risk of cardiovascular disease, type 2 diabetes and metabolic syndrome [Haffner and Taegtmeyer, 2003; Rubenstein, 2005], but only in the past few decades it became widely accepted that augmented body adiposity is a risk factor for several types of malignancies [Taubes, 2012; Vucenik and Stains, 2012]. Additionally, obesity can lead to worsened prognosis, poorer treatment outcome, and increased cancer-related deaths [Parekh et al., 2012].

Cutaneous melanoma incidence rates have increased in the last decades worldwide from 3% to 7% annually [Tuong et al., 2012].

These statistics suggest a doubling of rates every 10–20 years [Marks, 2000; Garbe and Leiter, 2009], raising melanoma to the most rapidly increasing cancer in Caucasians [Garbe and Leiter, 2009]. Several reports showed positive associations between increased body fat and the risk of cutaneous melanoma later in life [Dennis et al., 2008; Morpurgo et al., 2012; Nagel et al., 2012; Sergentanis et al., 2013], suggesting that the increasing incidence of melanoma may be related to the enlarged obesity prevalence.

In vivo adiposity-related stimulation of melanoma growth has been demonstrated [Brandon et al., 2009; Pandey et al., 2012; Wagner et al., 2012; Jung et al., 2015]. Tumour-associated macrophages [Wagner et al., 2012; Jung et al., 2015] and endothelial cells [Jung et al., 2015] have been pointed out as possible mediators in the growth-promoter effect of adipose tissue towards melanomas. In fact, tumour stroma comprises many different cell types, including fibroblasts, adipocytes, immune, and endothelial cells that, along with the extracellular matrix, are key players in cancer development and progression [Brychtova et al., 2011; Friedl and Alexander, 2011]. However, we hypothesize that adiposity might also exert a direct effect over melanocytes without the involvement of stromal cells in a paracrine or endocrine manner. Herein, we explored the biological role of adipocytes secretome in B16-F10 and MeWo melanoma cell survival and plasticity.

MATERIALS AND METHODS

CELL CULTURE AND IN VITRO TREATMENTS

The mouse melanoma B16-F10 cells exhibit in vitro a mixed morphology of spindle-shaped and epithelial-like cells. It was originally isolated from melanoma of the C57BL/6J mouse strain. B16-F10 is a metastatic variant of B16 melanomas with high tropism for lung invasion.

The human melanoma cell line MeWo was originally derived and established in culture from a lymph node metastasis from a 78-year-old male patient. MeWo is also a metastatic cell line. Similarly to B16-F10 it also resembles moderate lung invasion ability.

B16-F10 murine melanoma cell line (ATCC CRL-6475), MeWo human melanoma cells (ATCC HTB-65), and 3T3-L1 pre-adipocytes (ATCC CL-173) were maintained in Dulbecco′s modified eagle′s medium (DMEM; Sigma–Aldrich), Human dermal microvascular endothelial cells (HMEC-1, ATTC CRL-3243) were cultured in RPMI-1640 (Sigma–Aldrich) containing 10–ng/mL epidermal growth factor (BD Biosciences) and 1 μg/mL cortisone (Sigma–Aldrich). Both media formulations were supplemented with 10% heat-inactivated fetal bovine serum (FBS; Sigma–Aldrich), 1% penicillin/streptomycin/amphotericin B (Sigma–Aldrich). Cells were grown at 37°C under a humidified 5% CO_2 atmosphere. Cells were serum-deprived during 16 h before incubation with each treatment for every experiment. Unless otherwise specified, all treatments and controls were carried out in serum-free conditions.

ADIPOCYTE DIFFERENTIATION AND CONDITIONED MEDIUM COLLECTION

3T3-L1 pre-adipocytes were harvested and allowed to reach confluence. After 2 days (day 0), the differentiation was initiated by addition of a hormonal mixture composed of 2 μM insulin (Sigma–Aldrich), 1 μM dexamethasone (Sigma–Aldrich) and 0.25 mM isobutylmethylxanthine (Fluka) in complete medium. Three days later (day 3), the induction medium was replaced by complete medium supplemented with insulin only. At day 7, cultures with a differentiation yield higher than 80% were washed with phosphate buffered saline (PBS) and incubated in serum-free DMEM. After 24–h (day 8), the conditioned medium (CM) was harvested from the adipocytes cultures, spun for 5 min at 300*g* and the supernatant was stored at −80°C for the subsequent treatments.

ADIPOSE TISSUE ORGAN CULTURE

Fragments (8–10 mg) from visceral adipose tissue (VAT) and subcutaneous adipose tissue (SAT) depots were collected from 8-week-male C57BL/6J mice. The fragments were then washed with 1% penicillin/streptomycin/amphotericin B (Sigma–Aldrich) in PBS and cultured afterwards in 1 mL of DMEM supplemented with 10% FBS. The fragments were serum-deprived and 24–h later the CM harvested and centrifuged at 300*g* for 5 min.

MOUSE ADIPOKINE ARRAY ANALYSIS

Mouse adipokine antibody arrays (-# ARY-013; R&D systems) were performed using 1 mL of 3T3-L1, SAT, and VAT CM and following the manufacturer′s protocol. The pixel density of each spot was calculated with the microarray profiler plugin of the Image J software (NIH). The relative adipokine levels were calculated upon normalization with the adipokine levels of B16-F10 CM.

CELL VIABILITY ASSAY

To measure B16-F10 metabolic activity, after a 24 h incubation of 1×10^4 cells/mL with the different treatments, 20 μL of the MTS reagent, from CellTiter 96 Aqueous assay (Promega), was added into each 96-plate well followed by a 3 h incubation period. Color development was determined by measuring absorbance at 490 nm.

APOPTOSIS ASSAY

Terminal deoxynucleotidyl transferase-mediated deoxyuridine triphosphate nick-end labelling (TUNEL) assay was performed in B16-F10 cells (1×10^4 cells/mL), after 24 h incubation with the different treatments using the In Situ Cell Death Detection Kit (Roche Diagnostics) following the manufacturers protocol. Nuclei were counter-stained with DAPI (Roche Diagnostics) and immunofluorescence was visualized under a fluorescence microscope (Nikon). The percentage of TUNEL-positive cells was evaluated by counting the cells stained with TUNEL divided by the total number of DAPI-stained nuclei at a 200× magnification field. One thousand nuclei were evaluated. The results are presented as mean ± standard error of the mean (SEM).

BRDU PROLIFERATION ASSAY

B16-F10 cells (1×10^4 cells/mL) were cultured with standard treatments in serum-free conditions for 20 h. Then bromodeoxyuridine (BrdU; Roche Diagnostics), at a final concentration of 0.01 mM, was added to each well for 4 h. The detection was performed using the colorimetric Cell Proliferation ELISA, BrdU (Roche Diagnostics), according to the manufacturer′s instructions.

CELL SPREADING AND ADHESION DETERMINATION

To determine cell spreading and adhesion [Humphries, 2001], B16-F10 cells were re-suspended in the different treatments at a final concentration of 5×10^4 cells/mL, seeded in a 24-well microplate and allowed to adhere and spread for 3 h and then washed with PBS to remove non-adherent cells. Fixation was performed with 4% (w/v) p-formaldehyde in PBS. Afterwards, 200 μL of crystal violet 0.1% (w/v) was added to each well for 20 min and later washed with H_2O. To evaluate the morphologic parameters (cell area, sphericity, size, and perimeter), 1,000 cells were analyzed by CellProfiler software (Broad Institute) on photographs of random fields, for each treatment, captured under an inverted microscope (Nikon) at a 200× magnification. To determine cell adhesion, the above protocol was reproduced but only allowing cells to adhere for 30 min. Afterwards, crystal violet dye was solubilized in 100 μL 10% (v/v) acetic acid (Fluka) and the absorbance measured at 570 nm using a plate reader.

ADHESION TO ENDOTHELIUM EVALUATION

HMEC-1 cells were cultured in a 24-well microplate with glass coverslips and allowed to reach confluence. Media was aspirated and the monolayers were washed with PBS. Afterwards, 1×10^5 cells/mL B16-F10 cells, in the different treatments were added to the wells for 30 min. To remove non-adherent cells, the wells were washed with PBS. Fixation was performed with 4% (w/v) *p*-formaldehyde for 10 min. Coverslips were then stained with Giemsa′s stain, thoroughly washed in Sorensen′s phosphate buffer and mounted on a microscope slide. Using a light microscope (Nikon) the number of cells adherent to the endothelial monolayer were counted in five random fields.

MELANIN CONTENT DETERMINATION

B16-F10 cells (5×10^5 cells/mL), were incubated with the different treatments for 24 h. Following detachment with 0.5% trypsin, cell density was assessed on a haemocytometer. After 300*g* centrifugation for 10 min, the pellet was washed twice with PBS and the melanin was solubilized in 1.0 mL of 1M NaOH (Panreac) containing 10% (v/v) dimethyl sulfoxide (Merck). Next, the absorbance at 475 nm was recorded. Results represent the mean absorbance (±SEM) of 1×10^6 cells.

TRANSWELL MIGRATION

Migration capacity was quantified on 24-well plates with 8 μm-pore transwell inserts (BD Biosciences). B16-F10 cells (5×10^4 cells/mL) were harvested on inserts in serum-free medium and placed on wells containing the standard treatments plus 10% FBS for 24 h. Membranes were then stained with crystal violet 0.1% (w/v) and visualized under a light microscope (Nikon). Five random fields of each membrane were counted on the microscope (Nikon) at a 100× magnification.

INJURY ASSAY

To perform the injury assay, melanoma cells at confluence were scrapped from the culture dish using a pipette tip, which left a void space. Cells were then incubated for 24 h following the standard treatments. After this period, damage recovery was then visualized and photographed under an inverted microscope (Nikon) at a 200× magnification. The wound closure was determined by measuring the wound area and by subtracting this value from the initial void space (CellProfiler software; Broad Institute). Shown are the means values (±SEM) of nine measurements for each time point and condition.

MATRIGEL CULTURES

To perform Matrigel cultures, 24-well plates were coated with 250 μL per well of Matrigel Basement Membrane Matrix (Corning). Afterwards, B16-F10 (5×10^4 cells/mL) or MeWo (20×10^4 cells/mL) melanocytes harvested in the respective treatments were fed on top of the Matrigel layer. Cell growth was then monitored and photographed under an inverted microscope (Nikon) at a 200× magnification for 24 h.

SOFT-AGAR COLONY FORMATION

The bottom of each 12-well plate was coated with 2 mL of 0.5% agarose and DMEM 2X. After polymerization the wells were fed with 5×10^3 B16-F10 cells in 2 mL of 0.2% agar and DMEM 2X. The medium was changed every 2–3 days. After 15 days, the wells were stained with 0.01% crystal violet and photographed. The number and area of the colonies was assessed with ImageJ software (NIH).

HANGING-DROP CELL CULTURES

Generation of melanoma spheroids was conducted as previously described [Foty, 2011]. Briefly, 2.5×10^6 B16-F10 or MeWo cells/mL were collected in the respective treatments and pippeted to the lid of a 60 mm non-adhesive petri dish leaving 10 μL drops onto the bottom of the lid. The lids were inverted, placed on top of the PBS-filled bottom chamber of the dish and incubated for 3 days.

STATISTICAL ANALYSIS

Results are expressed as mean ± SEM. Data were analyzed with GraphPad Prism 6.0 (GraphPad Software Inc.). Differences between samples and parameters among two experimental groups were evaluated by Student′s *t*-test. When three or more conditions were evaluated, statistical analysis was conducted through one-way ANOVA with Sidak post-hoc test. Significance was set at $P < 0.05$.

RESULTS

3T3-L1 SECRETOME INCREASES MELANOCYTES SURVIVAL, PROLIFERATION AND MELANIN CONTENT, AND DECREASES APOPTOSIS

3T3-L1 preadipocytes are a commercially available cell line for studying adipogenesis [Green and Kehinde, 1975; Poulos et al., 2010]. Their differentiation, in culture, into mature adipocytes is well widespread and can be achieved by established protocols. We used CM from fully differentiated 3T3-L1 cells to explore the potential effects of adipocytes secretome over malignant melanoma B16-F10 cells viability, proliferation, and apoptosis.

We first analyzed the effects of this conditioned medium in melanoma cells viability by the MTS assay. After a 24 h exposure to adipocyte CM, melanoma cells showed a 48% increase in their

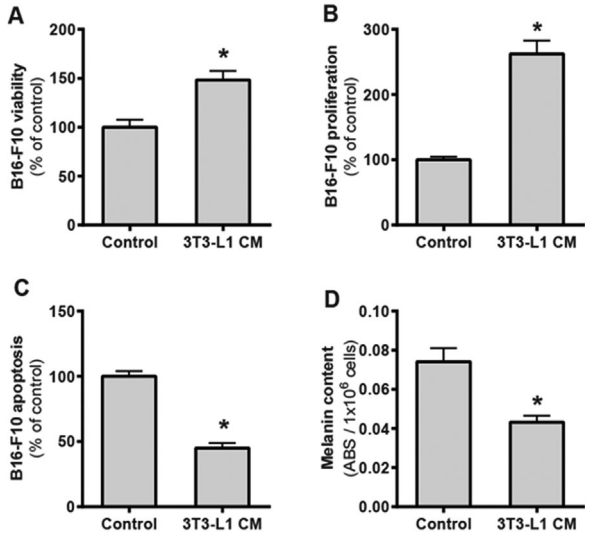

Fig. 1. 3T3-L1 secretome increases melanoma cell survival. B16-F10 cells were incubated with CM from differentiated 3T3-L1 cells cultures (3T3-L1 CM) or untreated (Control) for 24 h. (A) An increase in the percentage of viable melanoma cells was observed when compared with control. Results represent the percentage of viable cells normalized by the absorbance of control. (B) The number of proliferating cells, incorporating BrdU, increased in the presence 3T3-L1 CM. Results represent the percentage of proliferating cells normalized over the absorbance of control. (C) A significant decrease in the percentage of apoptotic cells was observed when melanocytes were treated with 3T3-L1 CM. Results represent the percentage of apoptotic cells evaluated by the ratios of TUNEL-positive cells versus total DAPI-counterstained nuclei. (D) The melanin content per cell was significantly decreased when melanocytes were cultured in presence of 3T3-L1 CM. Melanin concentration was calculated by determination of OD 475. Results represent the absorbance of 1×10^6 cells. ($^{*}P < 0.05$ vs. Control; $n = 9$).

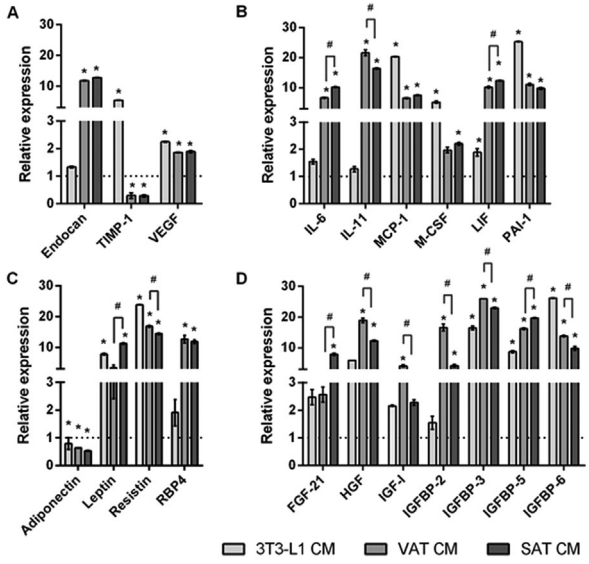

Fig. 2. Secretion profiles of 3T3-L1 cells and subcutaneous and visceral AT organ cultures. (A) Both SAT and VAT CM exhibit greater levels of VEGF and endocan with a concomitant reduction in the expression of TIMP-1. (B) Distinct relative levels of IL-6, IL-11, and LIF were found among SAT and VAT CM (C) Adipokines leptin and resistin are overexpressed in all CM, whereas diponectin levels are significantly reduced (D) Numerous cellular growth factors were present at considerably higher concentrations in both VAT and SAT CM ($^{*}P < 0.05$ vs. Control; $^{\#}P < 0.05$ SAT CM vs. VAT CM; $n = 2$).

metabolic activity (Fig. 1A). We found as well that the fraction of proliferating B16-F10 cells was significantly increased, as shown by the higher BrdU incorporation, in the presence of these adipocyte-released factors (Fig. 1B). The effect of 3T3-L1 secretome on apoptosis was examined using TUNEL analysis. Concomitantly, 3T3-L1 CM medium decreased B16-F10 programmed cell death by approximately 50% (Fig. 1C). These effects were further accompanied by a significant reduction in melanin content per cell (Fig. 1D).

ADIPOCYTE SECRETOME PROFILE CHARACTERIZATION

The previous findings imply that adipocytes released factors stimulate melanoma cell viability and aggressiveness. Therefore, we then assessed the secretion profile of adipocytes to further elucidate the involvement of adipose tissue in melanoma behavior (see Supplemental data). Given the well-established distinct biological and metabolic roles of sub-cutaneous (SAT) and visceral (VAT) adipose tissue, microarray assay was performed not only in 3T3-L1 cells, but also in organ cultures of SAT and VAT fragments.

As illustrated in Figure 2, the secretion patterns of numerous growth-factors, adipokines, cytokines, and angiogenesis-related molecules are different among the different CM. Greater levels of vascular endothelial growth factor (VEGF) and endocan were found in SAT and VAT CM, whereas tissue inhibitor of metalloproteinases-1 (TIMP-1) levels were significantly reduced in these two CM (Fig. 2A). On the other hand, 3T3-L1 CM exhibited higher levels of VEGF, TIMP-1, and endocan than B16-F10-CM (Fig. 2A). The levels of the interleukin (IL) family of cytokines: IL-6, IL-11, and leukaemia inhibitory factor (LIF) were also significantly overexpressed within SAT and VAT, although no substantial differences were found in the 3T3-L1 CM (Fig. 2B). Nonetheless, monocyte chemotactic protein 1 (MCP-1) and plasminogen activator inhibitor-1 (PAI-1) expression was upregulated in every CM (Fig. 2B). Adipose tissue hormones were also identified. Resistin and leptin relative expression levels were higher in 3T3-L1, SAT, and VAT CM. In addition, Retinol binding protein-4 (RBP-4) was significantly released in SAT and VAT, but not in 3T3-L1 CM. Interestingly enough, a significant reduction in adiponectin levels was observed in all CM (Fig. 2C). The levels of several growth factors involved both in metabolism and in cell behavior were also analyzed. VAT CM revealed the higher expression of fibroblast growth factor (FGF)-21, insulin-like growth factor binding protein (IGFBP)-5, whereas hepatocyte growth factor (HGF), insulin-like growth factor(IGF)-I, IGFBP-2, IGFBP-3, and IGFBP-6 levels were significantly higher in SAT than VAT CM (Fig. 2D).

SAT AND VAT DISTINCTIVELY MODULATE MELANOCYTE MIGRATION AND CELL SPREADING

According to the previous secretome profile, TIMP-1, an inhibitor of extracellular matrix degradation was significantly decreased, whereas several inflammatory cytokines and angiogenic growth factors were upregulated particularly in SAT and VAT. These findings led us to evaluate the influence of CM in melanocytes motility. We first analyzed whether 3T3-L1 CM mechanically induced a wound to B16-F10 confluent cultures by injury assay. As illustrated in Figure 3A, the resulting void area was promptly occupied by melanocytes upon 3T3-L1 CM incubation in comparison to untreated B16-F10 cultures. Following a 24 h incubation with CM, the migrated distance is almost twice the distance of the control treatment as seen by the microscopic examination of the wounds (Fig. 3B). We then examined the effect of SAT and VAT fat depots secretome in B16-F10 cells motility. In the double-chamber migration assay, the number of migrating cells following a chemotactic gradient was significantly enhanced in every treatment as compared to untreated B16-F10 cultures (Fig. 3C). However, SAT CM exerted this effect into a much larger extent. Cell spreading evaluation revealed that VAT and 3T3-L1 secreted molecules, but not SAT, induced spreading dynamic of B16-F10 cells (Fig. 3D). In addition, VAT CM-treated B16-F10 cells exhibited significantly higher areas and perimeter, whereas a smaller number of round shaped cells were observed. In contrast, SAT secreted factors did not significantly alter B16-F10 spread plasticity (Fig. 3E). These findings highlight a distinct paracrine role of AT depots regarding B16-F10 locomotive behavior: although SAT-released factors boost melanoma cell chemotaxis, VAT CM signalling enhance cell morphological plasticity and haptotactic spreading.

AT SECRETOME MODULATES MELANOMA CELLS ADHESION AND TUMORIGENESIS

Decreased cell–cell adhesion and anchorage-independent growth are prominent features necessary for successful metastization [Chiang and Massagué, 2008; Friedl and Alexander, 2011]. Therefore, we evaluated the adhesion of CM-treated B16-F10 cells to standard cell culture plates. Interestingly, B16-F10 cells adhesion was significantly increased after incubation with every CM, being higher upon VAT medium exposure (Fig. 4A).

Identical findings were observed in B16-F10 cells adhesion to endothelial cells (Fig. 4C). The number of B16-F10 cells adherent to

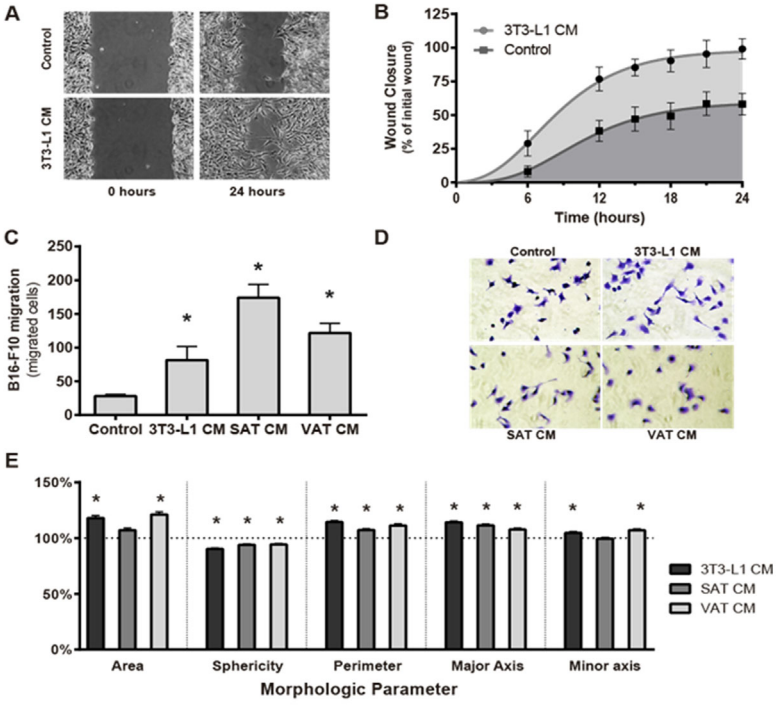

Fig. 3. In vitro motility, migration and spreading analysis of B16–F10 melanocytes. (A) A rapid B16–F10 cell migration was observed after incubation with 3T3–L1 CM in comparison to untreated (Control) for 24 h. Cell cultures were visualized under an inverted microscope at a 200× magnification. (B) When exposed to 3T3–L1 CM, melanocytes rapidly occupied the injury-created void area. The wound closure was determined by measuring cultures void area and by subtracting it from the initial area of the wound. Bars show the means values (±SEM) of nine measurements for each time point/condition. (C) The effects of AT secretome on cell migration were quantified in a double-chamber assay using FBS as a chemoattractant. The number of cells that invaded the membrane was significantly higher when treated with 3T3–L1, and particularly with SAT and VAT CM. Mean values (±SEM) of three independent measurements are shown ($^{*}P < 0.05$ vs. Control; $^{\#}P < 0.05$ SAT CM vs. VAT CM; $n = 3$). (D) B16–F10 cells were allowed to adhere and spread for 3 h in the standard treatments. Representative images of crystal-violet stained melanoma cells are shown (200X). (E) Morphologic analysis of B16–F10 cells revealed that VAT and 3T3–L1 CM significantly enhanced cell spreading. Bars are the means values ± SEM, represented as percentage of Control, of 1,000 evaluated cells ($^{*}P < 0.05$ vs. Control; $n = 9$).

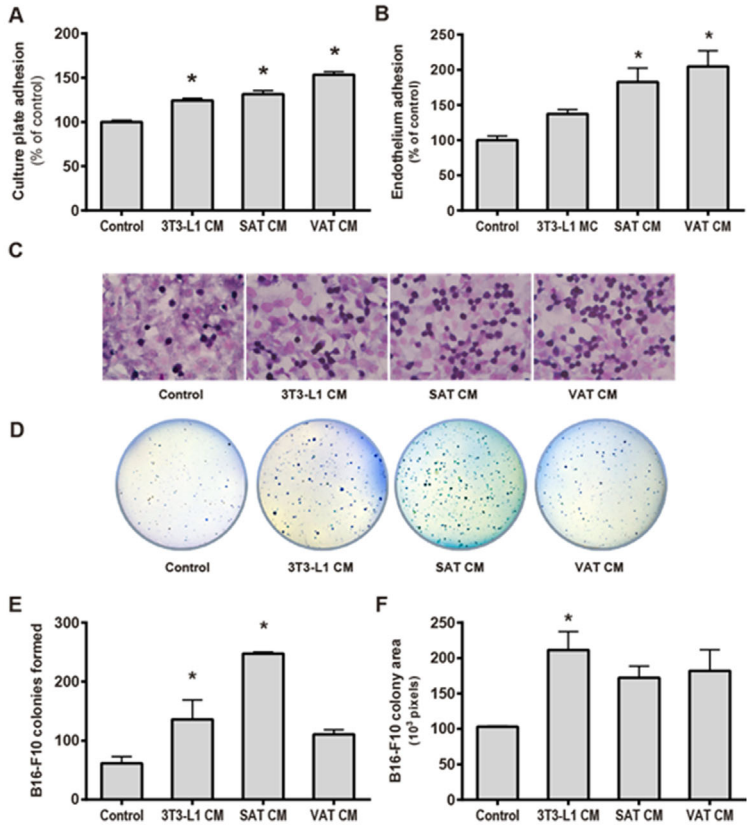

Fig. 4. Melanoma cells adhesion and anchorage-independent growth were increased after incubation with AT CM. (A) Adhesion to culture plates for 30 min; (B) Adhesion to HMEC-1 monolayers for 30 min. VAT-released factors were prominent in enhancing melanocytes adhesive potential both to culture plates and endothelial cells. Results are expressed as percentage of Control (±SEM). (C) Representative images (800X) of Giemsa stained slides showing B16-F10 cells (dark blue) adherent to HMEC-1 monolayers (pink). (D) Evaluation of anchorage-independent proliferation of B16-F10melanocytes was conducted by soft-agar colony formation assay. (E) The number of colonies formed was significantly higher in both 3T3-L1 and SAT CM treatments but not in VAT CM. (F) Mean B16-F10 colony area was significantly increased after 3T3-L1 CM incubation, but not after VAT or SAT CM treatment. Bars represent means ± SEM ($^{*}P < 0.05$ vs. Control; $^{\#}P < 0.05$ SAT CM vs. VAT CM; n = 3–9).

HMEC-1 monolayers was significantly enhanced both after SAT and VAT CM treatments as compared to untreated cells or to cells treated with 3T3-L1 CM (Fig. 4B), being the highest increase found upon VAT CM incubation. These findings confirm that VAT improves B16-F10 adhesive properties. Conversely, in the soft-agar clonogenic assay, SAT soluble factors promoted the anchorage-independent proliferation of B16-F10 cells upon culture in non-adherent conditions (Fig. 4D and E), whereas exposure to VAT CM did not exert any effect. SAT released factors increased the number of colonies formed, but not in a statistically significant manner (Fig. 4F). These results further emphasize the divergent roles of SAT and VAT towards melanocytes malignancy.

ADIPOCYTES SECRETED FACTORS INDUCE MALIGNANT MELANOCYTES VASCULOGENIC MIMICRY

Given that malignant melanomas are highly vascularized tumours [Pirraco et al., 2010; Chung and Mahalingam, 2014] and metastatic melanoma cells actively participate in tumour vascularization [Hendrix et al., 2003; Chung and Mahalingam, 2014], we next addressed whether CM from 3T3-L1 adipocytes prompted B16-F10 melanoma cells toward vasculogenic mimicry.

In comparison to untreated cells, 3T3-L1 CM-treated B16 cells rapidly assembled into capillary-like structures when cultured in Matrigel basement matrix (Fig. 5A). To further confirm the three-dimensional growth and spatial arrangement of the melanoma cells, B16-F10 cells were cultured in hanging-drops for 72 h. Microscopic observation of the generated spheroids upon incubation with 3T3-L1 CM revealed the formation of large and diffused aggregates of B16-F10 cells, whereas in the control treatment, a spherical and compact mass of melanocytes was observed (Fig. 5B). Next, we used MeWo cell line to additionally examine the vasculogenic mimicry inducer effects of 3T3-L1 CM in human melanoma cells. MeWo cells, when cultured on top of Matrigel and in the presence of 3T3-L1 CM displayed the same vessel-like rearrangement already observed for B16-F10 melanocytes (Fig. 5A). MeWo spheroids further revealed a loophole growth pattern when exposed to 3T3-L1-released factors (Fig. 5B). Altogether, these findings regarding cell–cell adhesion and reorganization into vessel-like structures formation provide additional

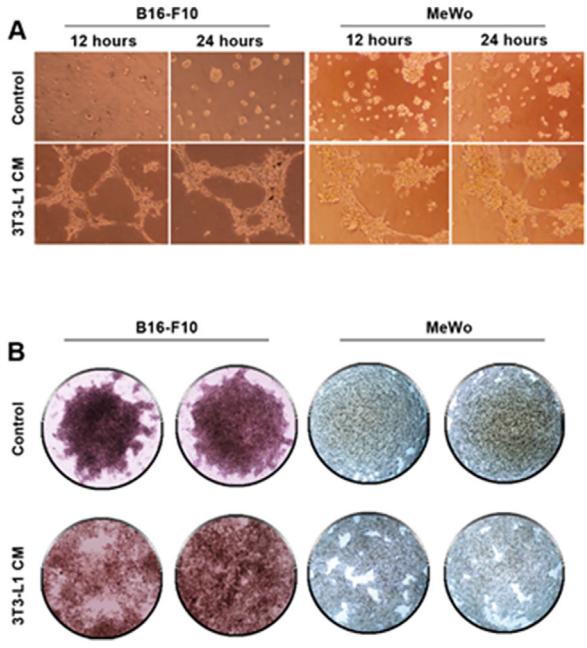

Fig. 5. Vasculogenic mimicry by melanoma cells was stimulated by AT CM. (A) B16-F10 and MeWo cells were cultured on top of Matrigel layers. Upon treatment with 3T3-L1 CM, melanocytes acquired a vessel-like tubular phenotype. Images were captured under an inverted microscope (200×) at 12 and 24 h post treatment. (B) Microscopic examination of B16-F10 and MeWo spheroids in hanging-drop cultures. The presence of 3T3-L1 secreted factors inhibited the formation of a compact spheroid cellular mass. Shown are representative light-microscopy photographs (80×) of the spheroids.

support and reinforce the deleterious effects of fat-secreted molecules on melanoma tumour progression.

DISCUSSION

Emerging evidence indicates that systemic factors, including inflammatory, angiogenic or metabolic markers, significantly influence tumour behavior [Hanahan and Weinberg, 2011].

The current study reveals that adipocyte-released factors increase B16-F10 melanoma cells viability, proliferation, and reduces apoptosis and melanin content. Exposure to adipose tissue CM of these cells further resulted in increased motility, enhancing the capacity to migrate and spread. These findings were accompanied by an augmented adhesion capacity, in particularly to endothelial cells, and anchorage-independent proliferation as assessed by soft agar assays. We further identified the factors that are released by adipocyte cells of different depots, and revealed that several pro-inflammatory factors (IL-6, IL-11, LIF, and PAI-1), metabolic markers (IGFBPs, FGF-21), angiogenic growth factors (endocan, HGF, VEGF IGF-I), and hormones (leptin, resistin, RBP-4) were secreted to the medium into a high extent, whereas TIMP-1, an inhibitor of ECM degradation, and adiponectin were significantly downregulated.

Adipose tissue is no longer considered a mere lipid store depot, but also an inflammatory and endocrine organ [Monteiro, 2009; Mendonça and Soares, 2015]. Accordingly, obesity provides a chronic low grade inflammatory condition, further potentiated by the presence of hormone cues and cytokines, which are strongly associated with disease. Therefore, the presence of high amounts of pro-inflammatory cytokines and hormones in adipocyte CM is expected. Remarkably, the majority of these factors are known to play a role in cell proliferation, apoptosis, migration, and invasiveness, as well as adhesion capacity. Recently, it has been reported that both leptin and resistin, two adipocyte-released hormones, were able to stimulate melanoma cell growth and proliferation through Akt and fatty acid synthase modulation [Malvi et al., 2015]. In addition to these hormones, FGF-21, a metabolic regulator also increases cell proliferation in vitro and increased tumorigenesis and invasive potential in vivo [Osawa et al., 2009]. Likewise, FGF and IL-6 are known to be produced by melanoma cells and stimulate proliferation in a autocrine manner, although other paracrine growth factors (HGF, IGF-I, and VEGF) modulate the microenvironment and potentiate tumor growth and invasion [Lázár-Molnár et al., 2000; Hoashi et al., 2001]. We have found that adipose tissues CM have significant higher levels of the above growth factors, reinforcing our findings concerning the effect of CM from the distinct adipose tissue depots studied in augmenting B16-F10 cell proliferation, migration, ability to invade, and decreasing apoptosis.

Along with the progression of melanoma, malignant melanocytes dedifferentiate losing most of their epithelial characteristics through a process similar to epithelial-mesenchymal transition [Fenouille et al., 2012], leading thus to more aggressive phenotypes [Thiery, 2002]. Melanogenesis is an inherent process in melanocytes. Melanocytes respond to the inflammatory cytokines, namely IL-6, with a dose-dependent inhibition of melanogenesis [Kotobuki et al., 2012]. Nevertheless, whenever these cells exhibit a more malignant phenotype, melanocytes decrease melanin synthesis [Jimbow et al., 1993]. Our findings show that when treated with CM from adipocytes, the melanin content per B16-F10 melanocyte was significantly reduced, further enlightening the growth-promoter and dedifferentiation paracrine effects of adipocytes.

Furthermore, active locomotion of tumour cells is fundamental to malignant invasive and metastatic capacity [Zhao et al., 2001; Fidler, 2003; Friedl and Wolf, 2003]. By crossing tissue stroma and the vascular bed, tumour cells interact with both extracellular matrix and soluble tropic factors. Our findings showed that chemotactic migration of B16-F10 cells was enhanced upon exposure to SAT-released factors although cell spreading and haptotactic migration of tumour cells were positively modulated by visceral-fat secretome. Intercellular adhesion is reduced in many aggressive tumours [Chiang and Massagué, 2008], allowing cells to detach from the primary lesion and metastasize to distant organs. Again, we found discrete effects among subcutaneous and visceral fat depots on B16-F10 adhesive properties. In fact, several biological, metabolic, and secretory differences distinguish intra-abdominal visceral-adipocytes from peripheral subcutaneous adipose tissue [Ibrahim, 2010; Ali et al., 2013]. In agreement, our results unveiled distinct effects of SAT and VAT upon melanocytes aggressiveness. SAT CM enhances B16-F10 locomotion and anchorage-independent proliferation. In turn, VAT prominently improves melanocytes cell-substratum adhesion. Despite the higher release of visceral-fat

pro-inflammatory cytokines [Ibrahim, 2010], subcutaneous fat depots, which are located close to melanoma lesions, influence the malignant transformation of melanocytes. Nevertheless, our microarray assay revealed that the secretome profile of SAT and VAT is significantly different regarding some of the inflammatory, hormonal, and metabolic molecules addressed. TIMP-1 and IGF-I are chemotactic agents for human melanoma cells that mediate motility [Hoashi et al., 2001; Neudauer and McCarthy, 2003]. IGF-I was significantly higher in SAT CM although TIMP-1 was under expressed in the adipose tissues CM. PAI-1 is also known to modulate cell adhesive properties and its overexpression is correlated with the metastatic capacity of melanomas [Quax et al., 1991]. Antagonistically, IGFBPs inhibit melanoma migratory and invasive behavior, and induce melanocytic differentiation [Naspi et al., 2014] counterbalancing the IGF-I effects and most likely contribute to the discrete differences observed between subcutaneous and visceral CM. The effect of the different AT depot secretome in tumour cells behavior is beyond the scope of this study, however, our results reinforce the need for additional molecular studies to investigate how SAT and VAT affect tumour progression.

Accumulating data point out mechanisms associating obesity to melanoma [Dennis et al., 2008; Brandon et al., 2009; Meeran et al., 2009; Morpurgo et al., 2012; Pandey et al., 2012; Chen et al., 2013]. Recent reports unveiled the involvement of high-fat diet-induced increased cytokines and angiogenic factors in the crosstalk between tumour cells and macrophages [Costa et al., 2007; Wagner et al., 2012; Jung et al., 2015; Mendonça et al., 2015]. Recruitment of the immune system cells, which release factors that enhance tumour plasticity and the maintenance of stromal microenvironment, has already been described for other malignancies [Fridman et al., 2012; Hanahan and Coussens, 2012]. In contrast, our in vitro results disclose a direct effect of adiposity on melanoma cells, without the influence of either tumour-associated cell-mediated immunity or endothelium.

Vascularization plays a central role in tumour development and progression. Besides angiogenesis, vasculogenic mimicry provides an alternative, angiogenic-independent tumour microcirculation [Maniotis et al., 1999; Hendrix et al., 2003; Ribatti et al., 2013]. Melanoma cell-lined vascular networks sustain a redundant blood supply required for both growth and metastasis [Maniotis et al., 1999; Ribatti et al., 2013]. The presence of these functional vascular channels by the tumour itself is a predictor of poor prognosis in human melanoma patients [Thies et al., 2001; Cao et al., 2013] and might circumvent the effectiveness of anti-vascular drugs and anti-angiogenic therapies [Loges et al., 2010]. Fully differentiated 3T3-L1 adipocytes CM were able to induce malignant melanocytes to rearrange on Matrigel cultures into vessel-like structures typically reported for endothelial cells [Kleinman and Martin, 2005]. Moreover, microscopic inspection of B16-F10 and MeWo spheroids, obtained by hanging-drop cultures, revealed the same pattern of vasculogenic mimicry observed in cultures of human melanoma cell lines [Maniotis et al., 1999; van der Schaft et al., 2004]. Data confirming melanoma angiogenesis stimulation by AT tropic factors has recently been highlighted [Wagner et al., 2012; Jung et al., 2015]. However, we report for the first time supporting evidence endorsing the potential adipocyte secretome inducer effects of tumour vasculogenic mimicry. Accordingly, several angiogenic growth factors were significantly higher in CM, including HGF and VEGF. HGF was involved in vascular mimicry of hepatocellular carcinoma [Lirdprapamongkol et al., 2012]. Additionally, VEGF signalling was found to be involved in vascular mimicry through activation of VEGFR1 expression in melanoma cells [Frank et al., 2011], explaining the increased capacity of melanoma cells to form vasculogenic structures after treatment with adipocyte CM. Endocan, in turn, is a new tumour invasion and angiogenic marker, being overexpressed in tumour vessels [Matano et al., 2014]. The fact that it is upregulated in both SAT and VAT conditioned medium may also explain the involvement of adipose tissues in tumour aggressiveness.

Altogether, our results indicate that adipocytes secretome induce malignant melanocytes aggressiveness. The synergic increase in melanocyte survival, adhesion, motility, and plasticity allied to the stimuli for cell–cell networks of vasculogenic mimicry patterns, support the deleterious effects that adiposity partakes directly in melanoma progression.

REFERENCES

Ali AT, Hochfeld WE, Myburgh R, Pepper MS. 2013. Adipocyte and adipogenesis. Eur J Cell Biol 92:229–236.

Berghöfer A, Pischon T, Reinhold T, Apovian CM, Sharma AM, Willich SN. 2008. Obesity prevalence from a European perspective: A systematic review. BMC Public Health 8:200.

Brandon EL, Gu JW, Cantwell L, He Z, Wallace G, Hall JE. 2009. Obesity promotes melanoma tumor growth: Role of leptin. Cancer Biol Ther 8:1871–1879.

Brychtova S, Bezdekova M, Hirnak J, Sedlakova E, Tichy M, Brychta T. 2011. Stromal microenvironment alterations in malignant melanoma. In: Murph M, editor. Research on melanoma—A glimpse into current directions and future trends. Czech Republic: InTech.

Cao Z, Bao M, Miele L, Sarkar FH, Wang Z, Zhou Q. 2013. Tumour vasculogenic mimicry is associated with poor prognosis of human cancer patients: A systemic review and meta-analysis. Eur J Cancer 49:3914–3923.

Chen J, Chi M, Chen C, Zhang XD. 2013. Obesity and melanoma: Exploring molecular links. J Cell Biochem 114:1955–1961.

Chiang AC, Massagué J. 2008. Molecular basis of metastasis. N Engl J Med 359:2814–2823.

Chung HJ, Mahalingam M. 2014. Angiogenesis, vasculogenic mimicry and vascular invasion in cutaneous malignant melanoma—Implications for therapeutic strategies and targeted therapies. Expert Rev Anticancer Ther 14:621–639.

Costa C, Incio J, Soares R. 2007. Angiogenesis and chronic inflammation: Cause or consequence? Angiogenesis 10:149–166.

Dennis LK, Lowe JB, Lynch CF, Alavanja MCR. 2008. Cutaneous melanoma and obesity in the agricultural health study. Ann Epidemiol 18:214–221.

Fenouille N, Tichet M, Dufies M, Pottier A, Mogha A, Soo JK, Rocchi S, Mallavialle A, Galibert MD, Khammari A, Lacour JP, Ballotti R, Deckert M, Tartare-Deckert S. 2012. The epithelial-mesenchymal transition (EMT) regulatory factor SLUG (SNAI2) is a downstream target of SPARC and AKT in promoting melanoma cell invasion. PLoS ONE 7:e40378.

Fidler IJ. 2003. The pathogenesis of cancer metastasis: The "seed and soil" hypothesis revisited. Nat Rev Cancer 3:453–458.

Foty R. 2011. A simple hanging drop cell culture protocol for generation of 3D spheroids. J Vis Exp 2720.

Frank NY, Schatton T, Kim S, Zhan Q, Wilson BJ, Ma J, Saab KR, Osherov V, Widlund HR, Gasser M, Waaga-Gasser AM, Kupper TS, Murphy GF, Frank MH. 2011. VEGFR-1 expressed by malignant melanoma-initiating cells is required for tumor growth. Cancer Res 71:1474–1485.

Fridman WH, Pagès F, Sautès-Fridman C, Galon J. 2012. The immune contexture in human tumours: Impact on clinical outcome. Nat Rev Cancer 12:298–306.

Friedl P, Alexander S. 2011. Cancer invasion and the microenvironment: Plasticity and reciprocity. Cell 147:992–1009.

Friedl P, Wolf K. 2003. Tumour-cell invasion and migration: Diversity and escape mechanisms. Nat Rev Cancer 3:362–374.

Garbe C, Leiter U. 2009. Melanoma epidemiology and trends. Clin Dermatol 27:3–9.

Green H, Kehinde O. 1975. An established preadipose cell line and its differentiation in culture. II. Factors affecting the adipose conversion. Cell 5:19–27.

Haffner S, Taegtmeyer H. 2003. Epidemic obesity and the metabolic syndrome. Circulation 108:1541–1545.

Hanahan D, Coussens LM. 2012. Accessories to the crime: Functions of cells recruited to the tumor microenvironment. Cancer Cell 21:309–322.

Hanahan D, Weinberg RA. 2011. Hallmarks of cancer: The next generation. Cell 144:646–674.

Hendrix MJC, Seftor EA, Hess AR, Seftor REB. 2003. Vasculogenic mimicry and tumour-cell plasticity: Lessons from melanoma. Nat Rev Cancer 3:411–421.

Hoashi T, Kadono T, Kikuchi K, Etoh T, Tamaki K. 2001. Differential growth regulation in human melanoma cell lines by TIMP-1 and TIMP-2. Biochem Biophys Res Commun 288:371–379.

Humphries M. 2001. Cell adhesion assays. Mol Biotechnol 18:57–61.

Ibrahim MM. 2010. Subcutaneous and visceral adipose tissue: Structural and functional differences. Obes Rev 11:11–18.

Jimbow K, Lee SK, King MG, Hara H, Chen H, Dakour J, Marusyk H. 1993. Melanin pigments and melanosomal proteins as differentiation markers unique to normal and neoplastic melanocytes. J Invest Dermatol 100:259S–268S.

Jung JI, Cho HJ, Jung YJ, Kwon S-H, Her S, Choi SS, Shin S-H, Lee KW, Park JHY. 2015. High-fat diet-induced obesity increases lymphangiogenesis and lymph node metastasis in the B16F10 melanoma allograft model: Roles of adipocytes and M2-macrophages. Int J Cancer 136:258–270.

Kleinman HK, Martin GR. 2005. Matrigel: Basement membrane matrix with biological activity. Semin Cancer Biol 15:378–386.

Kotobuki Y, Tanemura A, Yang L, Itoi S, Wataya-Kaneda M, Murota H, Fujimoto M, Serada S, Naka T, Katayama I. 2012. Dysregulation of melanocyte function by Th17-related cytokines: Significance of Th17 cell infiltration in autoimmune vitiligo vulgaris. Pigment Cell Melanoma Res 25:219–230.

Lázár-Molnár E, Hegyesi H, Tóth S, Falus A. 2000. Autocrine and paracrine regulation by cytokines and growth factors in melanoma. Cytokine 12:547–554.

Lirdprapamongkol K, Chiablaem K, Sila-Asna M, Surarit R, Bunyaratvej A, Svasti J. 2012. Exploring stemness gene expression and vasculogenic mimicry capacity in well- and poorly-differentiated hepatocellular carcinoma cell lines. Biochem Biophys Res Commun 422:429–435.

Loges S, Schmidt T, Carmeliet P. 2010. Mechanisms of resistance to anti-angiogenic therapy and development of third-generation anti-angiogenic drug candidates. Genes Cancer 1:12–25.

Malvi P, Chaube B, Pandey V, Vijayakumar MV, Boreddy PR, Mohammad N, Singh SV, Bhat MK. 2015. Obesity induced rapid melanoma progression is reversed by orlistat treatment and dietary intervention: Role of adipokines. Mol Oncol 9:689–703.

Maniotis AJ, Folberg R, Hess A, Seftor EA, Gardner LM, Pe′er J, Trent JM, Meltzer PS, Hendrix MJ. 1999. Vascular channel formation by human melanoma cells in vivo and in vitro: Vasculogenic mimicry. Am J Pathol 155:739–752.

Marks R. 2000. Epidemiology of melanoma. Clin Exp Dermatol 25:459–463.

Matano F, Yoshida D, Ishii Y, Tahara S, Teramoto A, Morita A. 2014. Endocan, a new invasion and angiogenesis marker of pituitary adenomas. J Neurooncol 117:485–491.

Meeran SM, Singh T, Nagy TR, Katiyar SK. 2009. High-fat diet exacerbates inflammation and cell survival signals in the skin of ultraviolet B-irradiated C57BL/6 mice. Toxicol Appl Pharmacol 241:303–310.

Mendonça F, Soares R. 2015. Obesity and cancer phenotype: Is angiogenesis a missed link? Life Sci 139:16–23.

Mendonça FM, de Sousa FR, Barbosa AL, Martins SC, Araújo RL, Soares R, Abreu C. 2015. Metabolic syndrome and risk of cancer: Which link? Metabolism 64:182–189.

Monteiro R. 2009. Chronic inflammation in the metabolic syndrome: Emphasis on adipose tissue. In: Soares R, Costa C, editors. Oxidative stress, inflammation and angiogenesis in the metabolic syndrome. Springer Netherlands: Dordrecht.

Morpurgo G, Fioretti B, Catacuzzeno L. 2012. The increased incidence of malignant melanoma in obese individuals is due to impaired melanogenesis and melanocyte DNA repair. Med Hypotheses 78:533–535.

Nagel G, Bjürge T, Stocks T, Manjer J, Hallmans G, Edlinger M, Häggström C, Engeland A, Johansen D, Kleiner A, Selmer R, Ulmer H, Tretli S, Jonsson H, Concin H, Stattin P, Lukanova A. 2012. Metabolic risk factors and skin cancer in the metabolic syndrome and cancer project (Me-Can). Br J Dermatol 167:59–67.

Naspi A, Panasiti V, Abbate F, Roberti V, Devirgiliis V, Curzio M, Borghi M, Lozupone F, Carotti S, Morini S, Gaudio E, Calvieri S, Londei P. 2014. Insulin-like-growth-factor-binding-protein-3 (IGFBP-3) contrasts melanoma progression in vitro and in vivo. PLoS ONE 9:e98641.

Neudauer CL, McCarthy JB. 2003. Insulin-like growth factor I-stimulated melanoma cell migration requires phosphoinositide 3-kinase but not extracellular-regulated kinase activation. Exp Cell Res 286:128–137.

Osawa T, Muramatsu M, Watanabe M, Shibuya M. 2009. Hypoxia and low-nutrition double stress induces aggressiveness in a murine model of melanoma. Cancer Sci 100:844–851.

Pandey V, Vijayakumar MV, Ajay AK, Malvi P, Bhat MK. 2012. Diet-induced obesity increases melanoma progression: Involvement of Cav-1 and FASN. Int J Cancer 130:497–508.

Parekh N, Chandran U, Bandera EV. 2012. Obesity in Cancer Survival. Annu Rev Nutr 32:311–342.

Pirraco A, Coelho P, Rocha A, Costa R, Vasques L, Soares R. 2010. Imatinib targets PDGF signaling in melanoma and host smooth muscle neighboring cells. J Cell Biochem 111:433–441.

Poulos SP, Dodson MV, Hausman GJ. 2010. Cell line models for differentiation: Preadipocytes and adipocytes. Exp Biol Med (Maywood) 235:1185–1193.

Quax PH, van Muijen GN, Weening-Verhoeff EJ, Lund LR, Dano K, Ruiter DJ, Verheijen JH. 1991. Metastatic behavior of human melanoma cell lines in nude mice correlates with urokinase-type plasminogen activator, its type-1 inhibitor, and urokinase-mediated matrix degradation. J Cell Biol 115:191–199.

Ribatti D, Nico B, Cimpean AM, Raica M, Crivellato E, Ruggieri S, Vacca A. 2013. B16-F10 melanoma cells contribute to the new formation of blood vessels in the chick embryo chorioallantoic membrane through vasculogenic mimicry. Clin Exp Med 13:143–147.

Rubenstein AH. 2005. Obesity: A modern epidemic. Trans Am Clin Climatol Assoc 116:103–111.

Sergentanis TN, Antoniadis AG, Gogas HJ, Antonopoulos CN, Adami HO, Ekbom A, Petridou ET. 2013. Obesity and risk of malignant melanoma: A meta-analysis of cohort and case-control studies. Eur J Cancer 49:642–657.

Taubes G. 2012. Unraveling the obesity-cancer connection. Science 335:28–32.

Thiery JP. 2002. Epithelial-mesenchymal transitions in tumour progression. Nat Rev Cancer 2:442–454.

Thies A, Mangold U, Moll I, Schumacher U. 2001. PAS-positive loops and networks as a prognostic indicator in cutaneous malignant melanoma. J Pathol 195:537–542.

Tuong W, Cheng LS, Armstrong AW. 2012. Melanoma: Epidemiology, diagnosis, treatment, and outcomes. Dermatol Clin 30:113–124.

van der Schaft DWJ, Seftor REB, Seftor E a, Hess AR, Gruman LM, Kirschmann D a, Yokoyama Y, Griffioen AW, Hendrix MJC. 2004. Effects of angiogenesis inhibitors on vascular network formation by human endothelial and melanoma cells. J Natl Cancer Inst 96:1473–1477.

Vucenik I, Stains JP. 2012. Obesity and cancer risk: Evidence, mechanisms, and recommendations. Ann N Y Acad Sci 1271:37–43.

Wagner M, Bjerkvig R, Wiig H, Melero-Martin JM, Lin R-Z, Klagsbrun M, Dudley AC. 2012. Inflamed tumor-associated adipose tissue is a depot for macrophages that stimulate tumor growth and angiogenesis. Angiogenesis 15:481–495.

Zhao W, Liu H, Xu S, Entschladen F, Niggemann B, Zänker KS, Han R. 2001. Migration and metalloproteinases determine the invasive potential of mouse melanoma cells, but not melanin and telomerase. Cancer Lett 162:49–55.